Desalination and Water Treatment
www.deswater.com
doi: 10.5004/dwt.2023.30063

314 (2023) 49–58
December

Preparation of electrospun double-layer PVDF:PMMA membrane non-woven nanofibers for desalination by membrane distillation process

Nawras N. Safi, Basma I. Waisi*

Department of Chemical Engineering, College of Engineering, University of Baghdad, Iraq,
emails: basmawaisi@coeng.uobaghdad.edu.iq (B.I. Waisi), nawras.safi1507d@coeng.uobaghdad.edu.iq (N.N. Safi)

Received 11 July 2023; Accepted 12 October 2023

ABSTRACT

The electrospun nanofiber membranes have gained considerable interest in desalination membrane distillation applications due to their high surface area, hydrophobicity and porosity, controllable pore size, and membrane thickness. A double-layer of non-woven nanofibers membranes was prepared via the electrospinning method using hydrophobic polymers. The first (base) layer was hydrophobic polyvinylidene fluoride (PVDF) based electrospun nanofibers. The second (top) layer was hydrophobic polymethyl methacrylate (PMMA) based electrospun nanofibers. A series of dual-layer non-woven nanofiber membranes with various PVDF:PMMA amount percentages were fabricated and characterized regarding their morphology and wetting using scanning electron microscopy and contact angle. This was implemented through a systematic framework for investigating and optimizing related parameters such as feed concentration, feed temperature, and feed flow rate on the permeate flux. Effect of various operating conditions, such as feed inlet temperature ranging between 35°C and 55°C, salt concentration (i.e., 70,000–210,000 ppm), and feed flow rates (i.e., 0.2, 0.4, and 0.6 L/min) on permeate flux has been investigated. The pure water permeate flux of the prepared membrane was enhanced by approximately 25 PVDF:75 PMMA. When operated under the best-specified conditions (i.e., 70 g/L, 0.6 L/min, and 55°C), the direct contact membrane distillation results for the 25 PVDF:75 PMMA membrane demonstrated that its salt rejection was greater than 99.757% with flux 44.192 kg/m^2·h and a permeate conductivity below 243 μS/cm.

Keywords: Desalination; Direct contact membrane distillation; Electrospinning; Non-woven nanofibers; Hydrophobic polymer

1. Introduction

Our world is facing a water and energy shortage. One-sixth of the world's population has no access to improved drinking water, and signs suggest that it is getting worse and will continue to do so unless corrective action is taken [1]. Water is a critical necessity for the utilization of humanity [2]. The technology is more widely applicable across various industries [3]. Increased water demand due to population growth in recent decades has prompted efforts to find a promising technology that can help overcome water scarcity problems [4]. Membrane distillation (MD) is considered a promising technology for separations accomplished by classical separation processes such as distillation or reverse osmosis (RO). MD has become a popular research area since it has the potential to tackle the shortage of water while using a relatively small amounts of high-grade energy [5]. As a common separation process, membrane distillation is considered a low-cost separation process that can utilize poor-quality waste and different energy sources such as geothermal and solar energy [6,7].

The term MD comes from the similarity with the conventional distillation process, so both technologies are

* Corresponding author.

based on the vapor-liquid equilibrium for separation. Both require the latent heat of evaporation for the phase change from liquid-to-liquid vapor, achieved by heating the feed solution [8]. In the MD process, the vapor molecules diffuse from the feed solution, pass through a highly porous hydrophobic membrane, and condense at the permeate side. A hydrophobic and highly porous membrane is essential in the MD process to separate feed and permeate sides as a physical barrier [9].

Compared to conventional approaches, membrane distillation considers low energy and cost, but the main disadvantages of these processes are relatively low permeate flux [10,11]. In MD, microporous membranes were utilized to prevent wetting. These pores of the membrane may be hydrophobic. Also, they would offer low mass transfer resistance, good thermal stability, and excellent chemical resistance. The hydrophobic polymer has been the public option, like membrane materials in membrane distillation, paying to non-wettability by the feeds of aqueous [12].

Electrospun nanofiber membranes have received increasing attention in the membrane distillation (MD) process due to their high porosity and interconnected open pores that can be prepared using many hydrophobic polymers [13–16]. Electrospinning is a cost-effective technique to form continuous fibers within a nanosized scale from natural and synthetic polymers under electrostatic forces [17]. The electrospun nanofibers have outstanding characterizations such as a vast surface area-to-volume ratio, flexibility in surface functionalities, intrinsically high porosity, fully interconnected pore structures, low hydraulic resistance, and ease of scalable synthesis [17,18]. The nanofiber membrane is fabricated via the electrospinning technique, in which a high-voltage power source charges a jet of fluid that flows through a capillary tube [19].

Polysulfone [20], polyethersulfone [21], polyvinylidene fluoride (PVDF) [22], polymethyl methacrylate (PMMA), and polyacrylonitrile are widely used for producing non-woven nanofibers membranes due to their high mechanical and chemical resistance [23,24]. Researchers have used electrospun nanofibers in various potential applications such as tissue engineering [25–27], photo voltaic cells [28,29], high-performance air filters [30], membranes for separation processes [31,32], sensors [33,34], advanced composites [35,36]. In water filtration applications [37]. Chiral separation and desalination [38] etc. Electrospun nanofibrous membranes have high porosity and large pore size with narrow pore-size distribution and large surface area. These properties are desirable for the MD process to produce high water vapor flux.

This project aims to prepare double-layer flat sheet membranes to find the pore size suitability non-wettability for MD application. It may be hydrophobic and excellent chemical resistance by electrospinning a top layer of PMMA non-woven nanofiber on a layer of PVDF non-woven nanofiber producing a double-layer PVDF:PMMA non-woven nanofiber membrane. The fabricated nanofibers membranes were characterized using scanning electron microscopy (SEM) and water contact angle and applied in direct contact membrane distillation (DCMD) applications to obtain high solute rejection and low conductivity.

2. Materials and methods

2.1. Materials

PMMA (Mwt. of 350,000 g/mol) has been harnessed for membrane fabrication and PVDF (Mwt. of 543,000 g/mol). PMMA and PVDF were chosen due to their excellent thermal and chemical stability, high hydrophobicity and abrasion resistance, and good properties against aging. N,N-dimethylformamide (DMF) (density of 0.948 g/cm^3) was used as a solvent to dissolve PMMA and PVDF. Sodium chloride (NaCl) was used to prepare the saline solution. All chemicals were purchased from Sigma-Aldrich, Germany.

2.2. Membranes fabrication

PVDF-based non-woven nanofibers membrane was prepared by electrospinning technique which is a stretching motion of polymer droplets to resolve surface tension in a high voltage electrostatic field. The setup of the basic electrospinning contains a syringe containing a polymer solution, a needle made of metal, a voltage power supply, also a collector [39,40]. First, the polymeric solutions were prepared by dissolving a certain amount of polymer in DMF to prepare solutions under continuous stirring for 5 h at 40°C until a homogeneous clear precursor solution was obtained.

The dope solution was then degassed to eliminate air bubbles. Then, the precursor solution was put in a plastic syringe and secured in a syringe pump. Next, a metal needle (inner diameter was 0.7 mm) was connected to the nozzle of the syringe. Next, the polymeric nanofiber was stretched through the tip of the metal needle with a flow rate of 2 mL/h and collected on the rotating drum (rotating speed of 130 rpm) by applying a high voltage.

The main fabricated nanofiber membranes were a pure 10 wt.% PVDF/DMF and a pure 30 wt.% PMMA/DMF. The other fabricated nanofiber membranes were double-layers of different amounts percentages of the two polymers PVDF:PMMA (25:75, 50:50, and 75:25). Firstly, the base layer of non-woven PVDF-based nanofibers membranes was fabricated by spinning a certain amount of 10 wt.% PVDF/DMF solution using a voltage of 22 kV. Then, a top layer of non-woven nanofibers was fabricated by spinning a certain amount of 30 wt.% PMMA/DMF precursor solution using a voltage of 25 kV. All the membranes were spun at the same process parameters; the distance between the needle and collector of 15 cm, the injection flow rate of 2 mL/h, and the speed of the collector speed of 130 rpm. All the fabricated fibers were prepared at humidity (20–30) at room temperature. All the fabricated membranes had a fiber pore of 200–1,000 μm. All the nanofibers membranes in this work were created using the electrospinning approach, which includes the pulling action of polymer droplets in a high voltage 22–25 kV electrostatic field.

2.3. Preparation of NaCl solution

The brine (feed solution) was prepared by weighing 70, 140, and 210 g of annular (sodium chloride NaCl, M 58.44, didactic) using a sensitive balance (KERN PLE 310-3N). Each sample was dissolved in 1 L of distilled water and

mixed using a magnetic stirrer (MR Hei-Standard). An electric conductivity meter (Model DDS 307, Made in Germany) measures the conductivity of distilled water and solutions.

2.4. Characterization of membranes

The surfaces structure and morphologies of the pure PVDF and the pure PMMA non-woven nanofiber membranes and the double-layers of PVDF:PMMA non-woven nanofibers before and after sodium chloride (NaCl) removal were visualized. An SEM is typically used to analyze the structural morphology of the membranes [41]. The fiber size distributions and average fiber diameter were obtained from the SEM images by measuring the fiber sizes of twenty fiber diameter measurements of each membrane sample using ImageJ software (National Institutes of Health, USA). Also, to investigate the surface hydrophobicity of the fabricated membranes, the contact angle of water drops using a contact angle analyzer (Theta Lite TL-101).

2.5. Experimental methods (DCMD performance)

Fig. 1 shows the schematic diagram of the experimental setup of the direct contact membrane distillation process. The run of the direct contact membrane distillation experiment was curried for about 5 h. In the DCMD process, the hot feed solution was introduced in the top side of the flat sheet prepared membrane by a peristaltic pump at a flow rate controlled by a control valve with and pressure gauge on the right side. At the same time, the vapor water was pass through the membrane due to the partial pressure driving force at the membrane's sides to with cold distillate, the cold distillate water with the vapor water circle in the bottom side from module also by a peristaltic pump at a flow rate controlled by a control valve with and pressure gauge in the left side. That pump is made in England, chiller and bath are carried handmade. Chiller at a maintained temperature of 10°C, the prepared seawater in a 500 mL glass tank was heated by a water bath for different temperatures such as (i.e., 35°C–65°C). The Flat sheet membrane module of DCMD was designed and constructed in Italy in an area of about 6 cm^2 × 6 cm^2, as shown in Fig. 2.

The module is made from silicones that withstand corrosion by the NaCl solution and has high heat transfer resistance. Each chamber has a thickness of 2 mm, length = 4 cm, and width = 4 cm.

The flow paths within the direct contact module were of parallel flow type. The inlet and outlet temperatures of the feed streams were measured by the concrete heating control system, as shown in Fig. 1. The measurements of the collected volume of the permeate flux during the DCMD operation were evaluated by the continuous change in the

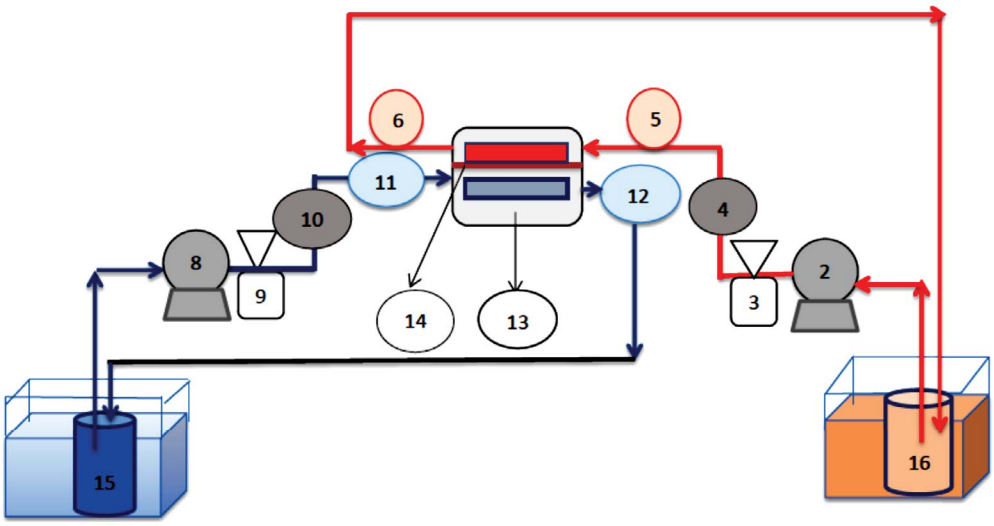

1.	Bath for feed	2.	Pump for feed
3.	Rotameter for feed	4.	Inlet pressure gauge for feed
5.	Inlet temperature sensor for feed	6	Outlet temperature sensor for feed
7.	Chiller for permeate mm	8.	Pump for chiller (permeate)
9.	Rotameter for chiller (permeate)	10.	Inlet pressure gauge for permeate
11.	Inlet temperature sensor for permeate	12.	Outlet temperature sensor for permeate
13.	Membrane module	14.	Membrane
15.	Tank for permeate	16.	Tank for feed

Fig. 1. Schematic diagram of the experimental rig for the direct contact membrane distillation process.

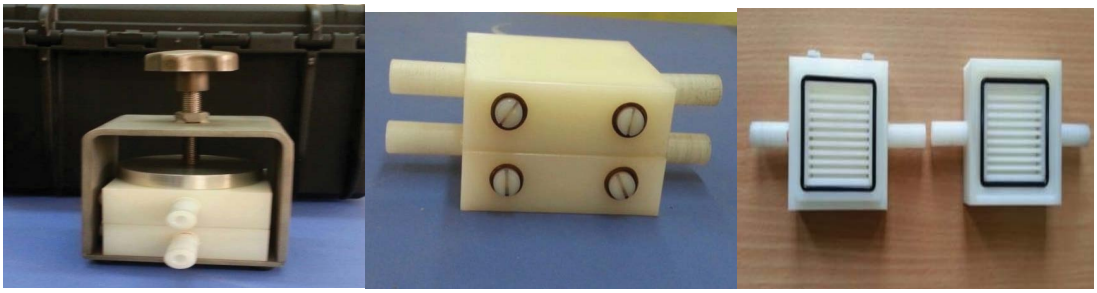

Fig. 2. Pictures of the membrane module from the outside and inside.

volume of the distilled water in the measuring cylinder. The salinity of the feed solution was kept constant by recycling the produced distilled water back to the feed tank. The permeate flux is evaluated in Eq. (1).

$$J_v = \frac{V \times \rho}{A \times t} \tag{1}$$

where J_v is water vapor permeation flux (kg/m^2·h), V is the volume of collected water (L), ϱ is water density (kg/m^3), A is the effective surface area of the membrane (m^2), and t is water collected time (h). The salt concentrations of the feed and permeate into and out of the membrane module were measured by a conductivity meter (Model DDS 307, Made in Germany) [42]. To calculate the salt rejection, the following equation was used:

$$R(\%) = \left[1 - \left(\frac{\mathrm{CP}}{\mathrm{CF}}\right)\right] \times 100 \tag{2}$$

where R is the salt rejection, CP is the concentration of permeates solution, and CF is the feed solution concentration [42].

In this work, the feed temperature ranged between 35°C and 55°C, and the DCMD performance was investigated in two steps. Step one tested the prepared membrane's performance of the one layer and double layer at various amounts, a feed at several temperatures (35°C, 45°C, and 55°C), using feed flow rate of 0.6 L/min with feed salt concentrations at 70 g/L) to carrying out the main experiments of saline water desalination.

The results of the permeate flux indicate that the optimal membranes were prepared from a (25 PVDF:75 PMMA). Additionally, three operating parameters, each at three levels, were adopted to estimate the water vapor flux. To reduce the number of experiments and select the best one used Taguchi technique requirements, nine experiments have been performed at disparate parameters, that is, the nine rows correspond to the number of the tests, with three columns representing the investigated parameters at three levels for each one, as given in Table 1. In the next stage, the membranes prepared at 30% from PMMA and 10% from PVDF (25 PVDF:75 PMMA) were examined in DCMD process at several feed temperatures (35°C, 45°C, 55°C, and 65°C), different feed salt concentrations (0, 70, 140, and 210 g/L), and various feed flow rates (0.2, 0.4, and 0.6 L/min) with Taguchi technique requirements at a group of minimal experiments.

Table 1
Direct contact membrane distillation experiments using Taguchi technique requirements (operating parameters)

Run	Feed temperature T (°C)	Feed concentration C (g/L)	Feed flow rate F (L/min)
1	35	70	0.2
2	35	140	0.4
3	35	210	0.6
4	45	70	0.4
5	45	140	0.6
6	45	210	0.2
7	55	70	0.6
8	55	140	0.2
9	55	210	0.4

3. Results and discussion

3.1. Membranes characterizations

Fig. 3 presents the images of surface morphologies of the fabricated pure PMMA/DMF and pure PVDF/DMF-based non-woven nanofibers membranes and the double-layers (PVDF:PMMA) non-woven nanofibers membranes at the various amounts of these two types of polymers. The images indicated that both PMMA/DMF and PVDF/DMF membranes were successfully fabricated. Homogeneous and continuous nanofibers were produced with average fiber diameters of 1,055.7 and 200.58 nm, respectively.

The PMMA pure non-woven nanofibers membranes were brittle fibers with large size fibers and pore size. To improve the properties of PMMA-based fibers membrane, it can be joined with strong fibers of small sizes and pore size like PVDF-based nanofibers producing double-layers non-woven nanofibers membranes.

The various double-layers (PVDF:PMMA) non-woven nanofibers membranes ((25:75), (50:50), and (75:25)) showed a mixture of fiber sizes confirming the existence of a layer of PVDF and a layer of PMMA in the membrane sheets which were successfully fabricated with average fiber diameters of 317.16, 444.21 and 567.72 nm, respectively. The small size PVDF-based fibers appeared in the bottom layer of the membrane, whereas the larger size of PMMA-based fibers formed a continuous top layer. Increasing the ratio of the PMMA in the dual-layer membrane increases the number of large fibers in the dual-layer membrane [31].

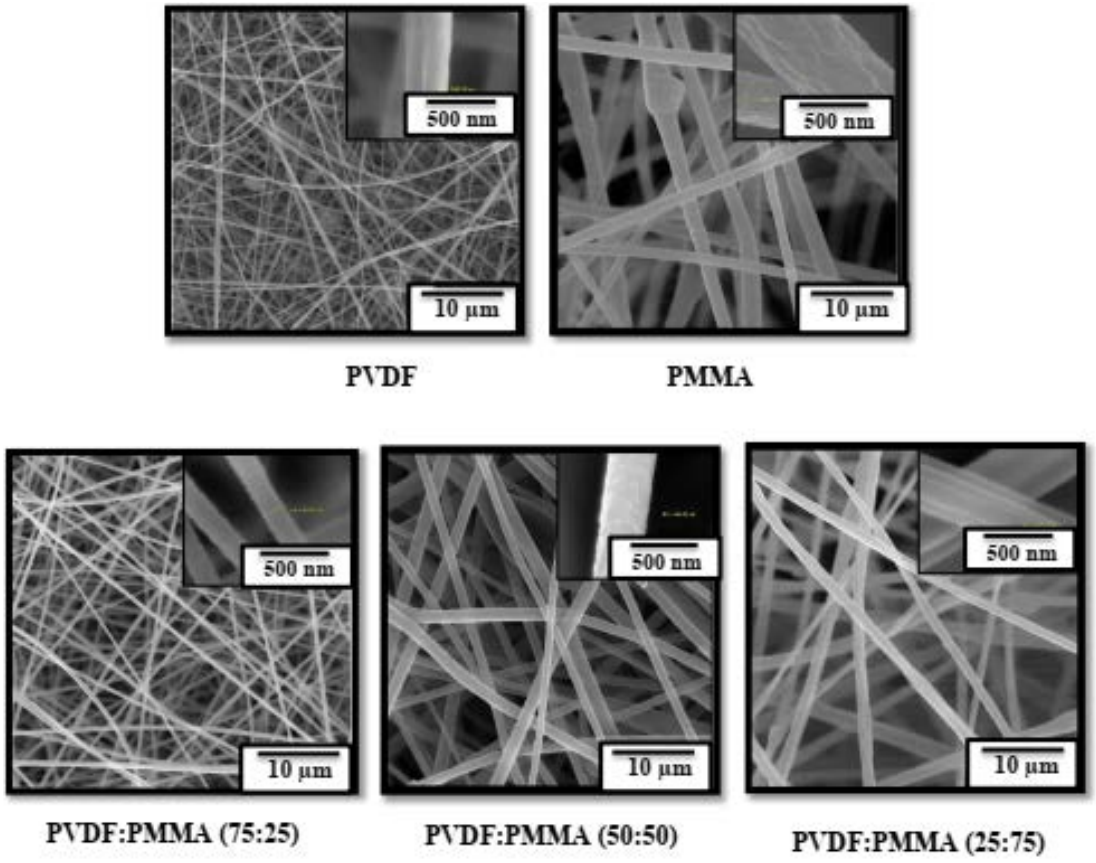

Fig. 3. Scanning electron microscopy of the prepared double-layers (PVDF:PMMA) non-woven nanofibers membranes before membrane distillation experiments with thickness (10 μm).

Whenever we increase a layer or percentage PMMA on the layer of PVDF with preserving the thickness, we notice an increase in fiber size from 200.58 nm of the pure PVDF to 317.16 nm (75 PVDF:25 PMMA), 444.21 nm (50 PVDF:50 PMMA) and 567.72 nm (25 PVDF:75 PMMA).

According to the average fiber diameters, all the prepared (pure and double layer) membranes were suitable for the MD system, whether before or after carried in the DCMD process. They all resulted in great results in flux and rejection.

The measured water contact angles also are summarized in Fig. 4 before and after MD. All nanofiber-prepared membranes recorded the successful value because of their best values to hydrophobicity suitable for MD. In contrast, the 25 PVDF:75 PMMA nanofiber membrane showed the highest contact angle due to its high hydrophobicity. As a result, spinning a top layer of the high hydrophobic PMMA-based nanofibers (120°) on the layer of high hydrophilic PVDF-based nanofibers (142°) caused a hydrophobic dual-layer nanofiber membrane (around 128°). The prepared water-repellent nanofibers in the same membrane increased hydrophobicity, which helped prevent the wetting of the membrane. The PVDF-based nanofiber membrane recorded the lowest value because of its high hydrophilicity. In contrast, due to its high hydrophobicity, the PMMA-based nanofiber membrane showed the highest contact angle [36]. As a result, spinning a top layer of the high hydrophobic PMMA-based nanofibers (136.2°) on the layer of high hydrophilic PVDF-based nanofibers (119.9°) caused a hydrophobic dual-layer nanofiber membrane 75:25 (around 125°), 50:50 (around 128.65°) and 25:75 (around 142.9°) increase the percentage of PMMA due to increase in hydrophobicity and contact angle.

Existing hydrophobic and hydrophobic nanofibers in the same membrane resulted in trapping the water in the micro and rough structure and passing only vapor due to an increase in the hydrophobicity and catching the saline droplets inside the hydrophobic fibers instead of clogging the membrane pores.

When comparing Table 2 characterizations of prepared membranes before and after the membrane distillation process, we saw that the percentage increase in fiber size expansion and the percentage decrease in contact angle are both at M_4, which is better because it indicates that the mechanical properties are better and stronger and that there is less wetting.

In Table 3, the results of prepared membranes noticed that M_5 has high flux but conductivity and concentration are high, and the rejection is less compared with M_1, M_2, and M_3 that be convergent in concentration and rejection but M_4 that be higher in flux from them with very close rates of conductivity, concentration and rejection with M_2 and M_3, it was chosen to be M_4 the best membrane among them as shown in Fig. 5. The results indicate the best

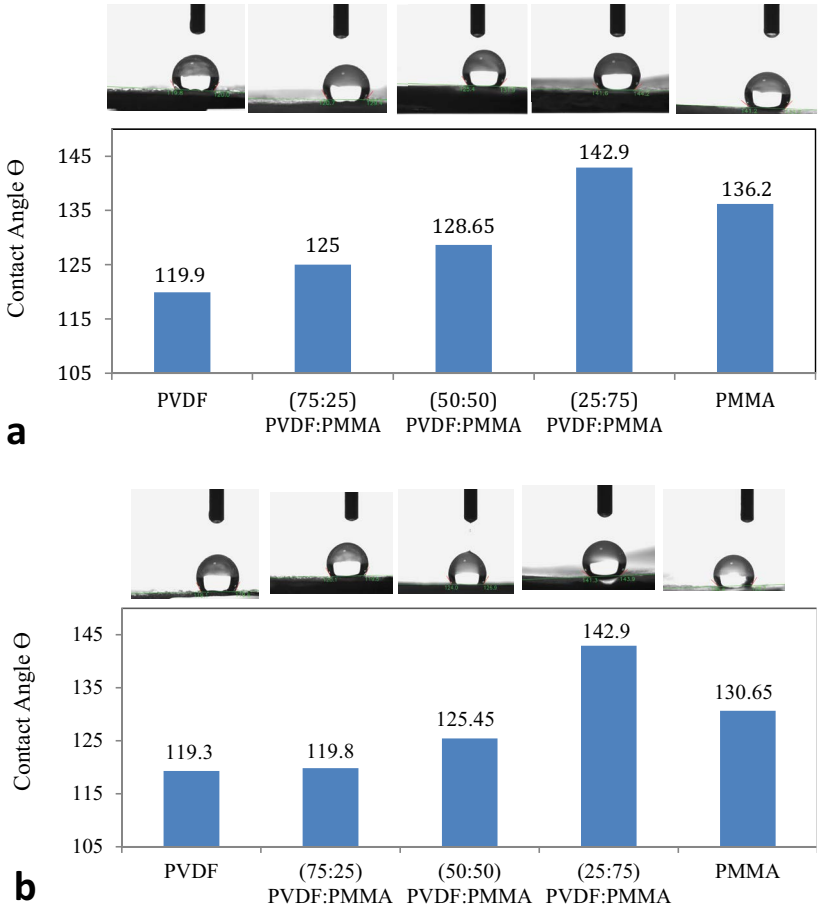

Fig. 4. Contact angle of the prepared double-layers (PVDF:PMMA) non-woven nanofibers membranes before and after membrane distillation experiments (a) before and (b) after membrane distillation.

Table 2
Characterizations of the prepared membranes

Polymer wt.%	Membrane name	Fiber size before MD	Fiber size after MD	Increase in pore size %	Contact angle before MD	Contact angle after MD	Decrease in contact angle %
PVDF 100%	M_1	200.58 ± 0.04	220.13 ± 0.03	8%	119.9 ± 0.52	119.3 ± 0.43	0.5
75 PVDF:25 PMMA	M_2	317.16 ± 0.02	332.61 ± 0.02	4%	125 ± 0.32	119.8 ± 0.25	4.4
50 PVDF:50 PMMA	M_3	444.21 ± 0.03	457.95 ± 0.03	3%	128.365 ± 0.22	125.45 ± 0.23	2.5
25 PVDF:75 PMMA	M_4	567.72 ± 0.01	579.31 ± 0.01	2%	142.9 ± 0.15	142.6 ± 0.11	0.2
PMMA 100%	M_5	1,055.7 ± 0.03	1,223.59 ± 0.02	14%	136.2 ± 0.35	130.65 ± 0.32	4.2

optimal membrane were choice prepared membrane from a M_4 in (25 PVDF:75 PMMA) which will be tested experimental in DCMD system and Taguchi method.

Taguchi method is a robust statistical design method founded to enhance the quality of manufactured goods. It has been introduced for the designing of experiments to probe how unlike parameters influence the variance and mean of any process performance characteristic that determines how good the process is functioning. The technique minimizes the process variation via the robust design of experiments [43]. According to the Taguchi design, an L9(3^4) orthogonal array (three variables in three levels) was examined. The results of the experiments are shown in Table 4 for flux and rejection prepared membrane at (25 PVDF:75 PMMA). The flux was measured after nearly 180 min. The better the performance characteristics, the greater the permeate flux. The influence of each parameter on the permeate flux in the DCMD process is shown in Table 4.

Since the experimental design is orthogonal, the role of each operating parameter on the major effect (permeate flux) at different levels could be separated. Table 4 manifested the response value for each level for prepared membranes. It can be seen that the maximum permeate flux was at 70 g/L, 0.6 L/min, and 55°C is 44.192 kg/m^2·h for the

Table 3
Distillation efficiency in direct contact membrane distillation process of prepared membranes (70 g/L feed concentration at 55°C feed temperature and 0.6 L/min feed flow rate)

Membrane name	Flux (kg/m²·h)	Concentration (g/L)	Conductivity (μS/cm)	Rejection (%)
M_1	13	0.105	137	99.850
M_2	20.120	0.161	230	99.770
M_3	26.512	0.168	238	99.760
M_4	44.192	0.170	243	99.757
M_5	45.138	0.660	634	99.057

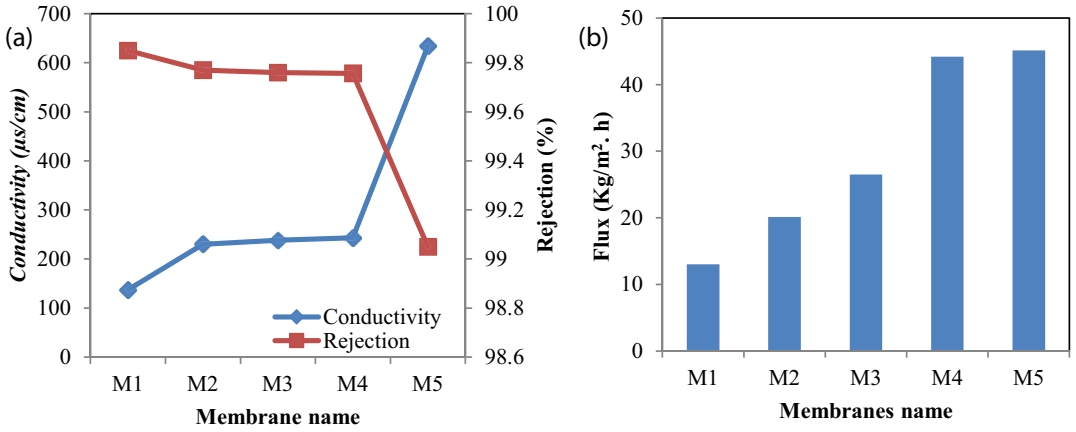

Fig. 5. Effect of different membranes on (a) flux, (b) conductivity, and rejection at 70 g/L feed concentration at 55°C feed temperature and 0.6 L/min feed flow rate.

Table 4
Taguchi L9(3^4) OA, and the result of experiments for prepared membrane (M_2). At 70 g/L feed concentration, 55°C feed temperature, and 0.6 L/min feed flow rate

Run	Feed temperature *T* (°C)	Feed concentration *C* (g/L)	Feed flow rate *F* (L/min)	Flux (kg/m²·h)	Rejection %
1	35	70	0.2	19.521 ± 0.2	99.856
2	35	140	0.4	18.631 ± 0.3	99.857
3	35	210	0.6	16.522 ± 0.2	99.851
4	45	70	0.4	28.341 ± 0.1	99.762
5	45	140	0.6	27.131 ± 0.1	99.764
6	45	210	0.2	23.553 ± 0.1	99.760
7	55	70	0.6	44.192 ± 0.2	99.757
8	55	140	0.2	33.829 ± 0.2	99.759
9	55	210	0.4	30.515 ± 0.1	99.760

prepared membrane, which represents the best operating conditions for these experiments (better performance characteristic). It shows the main effect plots based on the average values of each experimental run for system permeation flux. The reasonable trend of permeate flux, concerning the corresponding operating conditions, through the imaginary line, we note that the effect has indicated that the mean of means increased with increasing feed temperature and feed flow rate. In the meantime, it decreased with increasing feed concentration, as shown in Fig. 6. The figure has also represented the contribution of each parameter of operating conditions on the permeate flux. It can be concluded that the feed temperature was the most significant factor, while the feed flow rate showcased the lowest influence on the permeate flux. An empirical correlation for permeation flux as a function of operating variables, feed temperature (*T*), feed flow rate (*F*), and feed concentration (*C*) was obtained using the computer programs software "Minitab" Version 17 as following regression equation with *R*-sq. = 96.08%.

$$\text{Flux} = -9.97 + 0.8977T - 0.0511C + 9.12F \quad (3)$$

From the advantages of MD, the fouling of the membrane is less compared with revers osmose RO because of

Fig. 6. Effect of operating variables on mean of means: (a) feed temperature, (b) concentration and (c) feed flow rate.

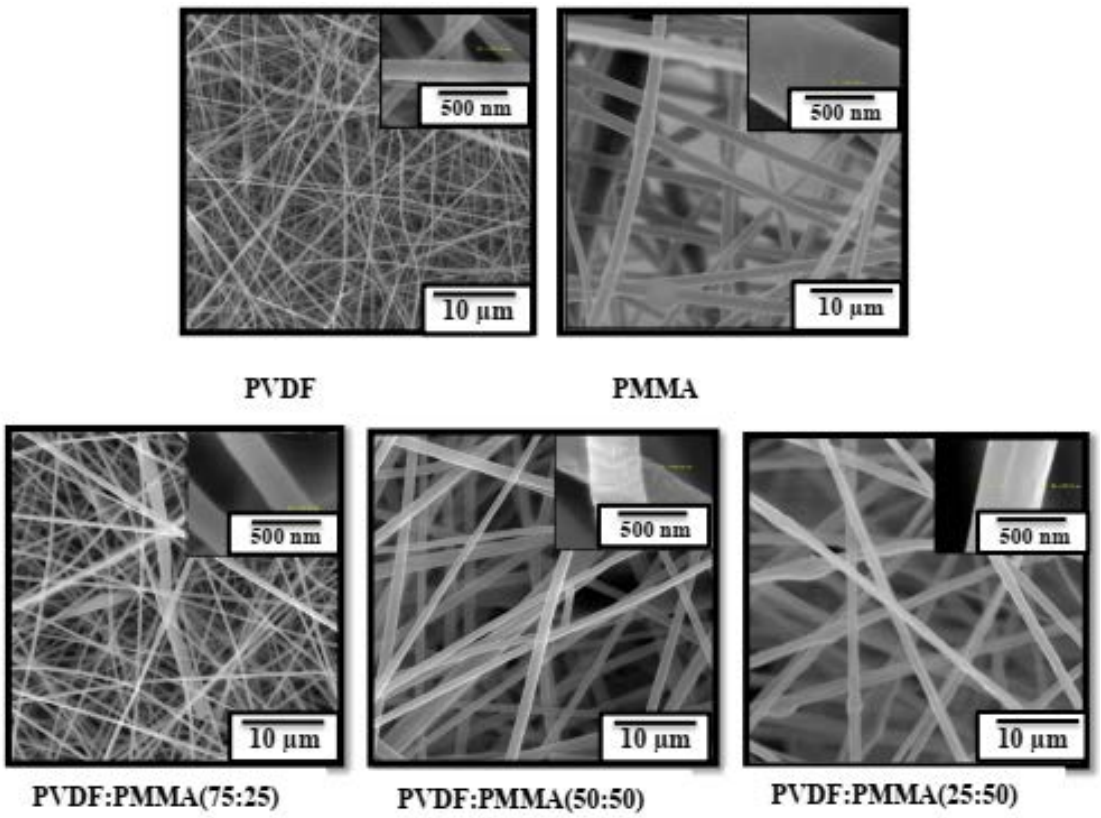

Fig. 7. Scanning electron microscopy of the prepared double-layers (PVDF:PMMA) non-woven nanofibers membranes after membrane distillation experiments.

larger pores and the hydrophobic nature of the membrane. However, slight wetting results from less pore or fiber size expansion at high temperatures. Fig. 7 shows the SEM of the prepared double-layers (PVDF:PMMA) non-woven nanofibers membranes after MD experiments. The images indicated that both 30 wt.% PMMA/DMF and 10 wt.% PVDF/DMF membranes with average fiber diameters after the DCMD process became about 1,223.59 and 220.13 nm, respectively. The various double-layers (PVDF:PMMA) non-woven nanofibers membranes ((25:75), (50:50), and (75:25)) showed average fiber diameters suitable for MD after this process became about 579.31, 457.95, and 332.61 nm, respectively because the simple expend the fiber at the hot solution.

4. Conclusions

This work successfully fabricated dual-layer nanofiber membranes with high organic wetting via electrospinning. The fabricated membrane consisted of a top layer of the hydrophobic PMMA nanofibers spun on the hydrophobic PVDF nanofibers membrane base layer. The characterization analysis of the fabricated membranes showed the high effect of the spinning nanofiber layer of PMMA on the base layer of PVDF, including the fiber size and wettability. The various prepared membranes were tested in membrane distillation desalination using a DCMD system. The dual-layer nanofibers membranes significantly improved permeate flux, wetting resistance, and high rejection. The flat membrane sheet to apply membrane distillation was successfully produced with various concentrations. Sweeping gas membrane distillation performance of M_4 was significantly improved. The best permeate flux (44.192 kg/m^2·h) by a solution of 70 g/L at 55°C feed temperature and 0.6 L/min feed flow rate was gained at (75 PMMA:25 PVDF) concentration with the best conductivity of about 243 μS/cm and rejection 99.757%. The permeation flux raises with the raising temperature of feed and feed flow rate and decreases with the increasing NaCl concentration. The feed temperature is the most effective factor, and the flow feed rate was the lowest effective factor on the permeation flux.

References

[1] L. Francis, H. Maab, A. AlSaadi, S. Nunes, N. Ghaffour, G.L. Amy, Fabrication of electrospun nanofibrous membranes for membrane distillation application, Desal. Water Treat., 51 (2013) 1337–1343.

[2] M.A.Z. Basma, A. Abdul Majeed, Performance study of electrodialysis for treatment fuel washing wastewater, Iraqi J. Chem. Pet. Eng., 17 (2016) 35–42.

[3] A. Faiq Al-Alawy, S. Mohsin Al-Musawi, Microfiltration membranes for separating oil/water emulsion, Iraqi J. Chem. Pet. Eng., 14 (2013) 53–70.

[4] M.R.S. Kebria, A. Rahimpour, S.K. Salestan, S. Fatemeh Seyedpour, A. Jafari, F. Banisheykholeslami, N. Tavajohi Hassan Kiadeh, Hyper-branched dendritic structure modified PVDF electrospun membranes for air gap membrane distillation, Desalination, 479 (2020) 114307, doi: 10.1016/j.desal.2019.114307.

[5] H.Y. Wu, R. Wang, R.W. Field, Direct contact membrane distillation: an experimental and analytical investigation of the effect of membrane thickness upon transmembrane flux, J. Membr. Sci., 470 (2014) 257–265.

[6] M.S. El-Bourawi, Z. Ding, R. Ma, M. Khayet, A framework for better understanding membrane distillation separation process, J. Membr. Sci., 285 (2006) 4–29.

[7] A.S. Khalaf, A.A. Hassan, A comparison study of brine desalination using direct contact and air gap membrane distillation, J. Eng., 25 (2019) 47–54.

[8] O. Pelin, Membrane Distillation: Principle, Advances, Limitations and Future Prospects in Food Industry, Z. Sina, Ed., Distillation, InTechOpen, Rijeka, 2012.

[9] J. Ju, K. Fejjari, Y. Cheng, M. Liu, Z. Li, W. Kang, Y. Liao, Engineering hierarchically structured superhydrophobic PTFE/POSS nanofibrous membranes for membrane distillation, Desalination, 486 (2020) 114481, doi: 10.1016/j.desal.2020.114481.

[10] M.M. Teoh, T.-S. Chung, Membrane distillation with hydrophobic macrovoid-free PVDF–PTFE hollow fiber membranes, Sep. Purif. Technol., 66 (2009) 229–236.

[11] A.A. Alcheikhhamdon, N.A. Darwish, N. Hilal, Statistical analysis of air-gap membrane desalination experimental data: hypothesis testing, Desalination, 362 (2015) 117–125.

[12] S. Shukla, N.E. Benes, I. Vankelecom, J.P. Méricq, M.P. Belleville, N. Hengl, J.S. Marcano, Sweep gas membrane distillation in a membrane contactor with metallic hollow-fibers, J. Membr. Sci., 493 (2015) 167–178.

[13] B.S. Lalia, E. Guillen-Burrieza, H.A. Arafat, R. Hashaikeh, Fabrication and characterization of polyvinylidenefluoride-co-hexafluoropropylene (PVDF-HFP) electrospun membranes for direct contact membrane distillation, J. Membr. Sci., 428 (2013) 104–115.

[14] H. Ke, E. Feldman, P. Guzman, J. Cole, Q. Wei, B. Chu, A. Alkhudhiri, R. Alrasheed, B.S. Hsiao, Electrospun polystyrene nanofibrous membranes for direct contact membrane distillation, J. Membr. Sci., 515 (2016) 86–97.

[15] M. Essalhi, M. Khayet, Self-sustained webs of polyvinylidene fluoride electrospun nanofibers at different electrospinning times: 1. Desalination by direct contact membrane distillation, J. Membr. Sci., 433 (2013) 167–179.

[16] B.I. Waisi, Carbonized co-polymers non-woven nanofibers composite: surface morphology and fibers orientation, Iraqi J. Chem. Pet. Eng., 20 (2019) 11–15.

[17] H.S. Al-Okaidy, B.I. Waisi, The effect of electrospinning parameters on morphological and mechanical properties of PAN-based nanofibers membrane, Baghdad Sci. J., (2023), doi: 10.21123/bsj.2023.7309.

[18] H. Sabeeh, B.I. Waisi, Effect of solvent type on PAN-based non-woven nanofibers membranes characterizations, Iraqi J. Chem. Pet. Eng., 23 (2022) 43–48.

[19] I. Alghoraibi, S. Alomari, Different Methods for Nanofiber Design and Fabrication, Springer INdAM Ser., 2018.

[20] Y. Aguilar-Costumbre, J.A. Lambert, M.A. Meléndez-Lira, V.A. Escobar-Barrios, Preparation of Membranes Based on Polysulfone (PSU) and Graphene Oxide (GrO) by Electrospinning, A. Maciel-Cerda, Ed., Membranes: Materials, Simulations, and Applications, Springer Int. Pub., Cham, 2017, pp. 23–30.

[21] L. Liu, F. Shen, B. Zhang, H. Jiang, J. Li, J. Luo, H. Wu, R. Khan, Y. Wan, Fabrication of PES-based membranes with a high and stable desalination performance for membrane distillation, RSC Adv., 6 (2016) 107840–107850.

[22] F.A. AlMarzooqi, M.R. Bilad, H.A. Arafat, Development of PVDF membranes for membrane distillation via vapour induced crystallisation, Eur. Polym. J., 77 (2016) 164–173.

[23] P.S. Suja, C.R. Reshmi, P. Sagitha, A. Sujith, Electrospun nanofibrous membranes for water purification, Polym. Rev., 57 (2017) 467–504.

[24] M. Al-Furaiji, J.T. Arena, J. Ren, N. Benes, A. Nijmeijer, J.R. McCutcheon, Triple-layer nanofiber membranes for treating high salinity brines using direct contact membrane distillation, Membranes, 9 (2019) 60, doi: 10.3390/membranes9050060.

[25] L. Francis, J. Venugopal, M.P. Prabhakaran, V. Thavasi, E. Marsano, S. Ramakrishna, Simultaneous electrospin–electrosprayed biocomposite nanofibrous scaffolds for bone tissue regeneration, Acta Biomater., 6 (2010) 4100–4109.

[26] J.A. Matthews, G.E. Wnek, D.G. Simpson, G.L. Bowlin, Electrospinning of collagen nanofibers, Biomacromolecules, 3 (2002) 232–238.

[27] C.Y. Xu, R. Inai, M. Kotaki, S. Ramakrishna, Aligned biodegradable nanofibrous structure: a potential scaffold for blood vessel engineering, Biomaterials, 25 (2004) 877–886.
[28] L. Francis, A. Sreekumaran Nair, R. Jose, S. Ramakrishna, V. Thavasi, E. Marsano, Fabrication and characterization of dye-sensitized solar cells from rutile nanofibers and nanorods, Energy, 36 (2011) 627–632.
[29] C. Drew, X. Wang, K. Senecal, H. Schreuder-Gibson, J. He, J. Kumar, L.A. Samuelson, electrospun photovoltaic cells, J. Macromol. Sci. A, 39 (2002) 1085–1094.
[30] M.G. Hajra, K. Mehta, G.G. Chase, Effects of humidity, temperature, and nanofibers on drop coalescence in glass fiber media, Sep. Purif. Technol., 30 (2003) 79–88.
[31] P. Gibson, H. Schreuder-Gibson, D. Rivin, Transport properties of porous membranes based on electrospun nanofibers, Colloids Surf., A, 187–188 (2001) 469–481.
[32] Z. Ma, M. Kotaki, S. Ramakrishna, Electrospun cellulose nanofiber as affinity membrane, J. Membr. Sci., 265 (2005) 115–123.
[33] X. Wang, C. Drew, S.-H. Lee, K.J. Senecal, J. Kumar, L.A. Samuelson, Electrospun nanofibrous membranes for highly sensitive optical sensors, Nano Lett., 2 (2002) 1273–1275.
[34] X. Wang, Y.G. Kim, C. Drew, B.C. Ku, J. Kumar, L.A. Samuelson, Electrostatic assembly of conjugated polymer thin layers on electrospun nanofibrous membranes for biosensors, Nano Lett., 4 (2004) 331–334.
[35] M.M. Bergshoef, G.J. Vancso, Transparent nanocomposites with ultrathin, electrospun nylon-4,6 fiber reinforcement, Adv. Mater., 11 (1999) 1362–1365.
[36] J.-s. Kim, D.H. Reneker, Mechanical properties of composites using ultrafine electrospun fibers, Polym. Compos., 20 (1999) 124–131.
[37] S.M. Alkarbouly, B.I. Waisi, Fabrication of electrospun nanofibers membrane for emulsified oil removal from oily wastewater, Baghdad Sci. J., 19 (2022) 1238–1238.
[38] K.C. Khulbe, T. Matsuura, Art to use electrospun nanofibers/nanofiber-based membrane in wastewater treatment, chiral separation and desalination, J. Membr. Sci. Res., 5 (2019) 100–125.
[39] M. Al-Furaiji, M. Kadhom, K. Kalash, B. Waisi, N. Albayati, Preparation of thin-film composite membranes supported with electrospun nanofibers for desalination by forward osmosis, Drinking Water Eng. Sci., 13 (2020) 51–57.
[40] B.I. Waisi, S.M. Al-Jubouri, J.R. McCutcheon, Fabrication and characterizations of silica nanoparticle embedded carbon nanofibers, Ind. Eng. Chem. Res., 58 (2019) 4462–4467.
[41] W. Zhou, R. Apkarian, Z.L. Wang, D. Joy, Fundamentals of Scanning Electron Microscopy (SEM), W. Zhou, Z.L. Wang, Eds., Scanning Microscopy for Nanotechnology, Springer, New York, NY, 2006. Available at: https://doi.org/10.1007/978-0-387-39620-0_1
[42] Q. Alsalhy, S. Ibrahim, S. Alkurwi, Seawater Desalination by Vacuum Membrane Distillation (VMD), The 2nd Arab Water Conference and Exhibition, AOAD, Doha, 2014, pp. 56–66.
[43] N.N. Safi, S.S. Ibrahim, N. Zouli, H.S. Majdi, Q.F. Alsalhy, E. Drioli, A. Figoli, A systematic framework for optimizing a sweeping gas membrane distillation (SGMD), Membranes (Basel), 10 (2020) 254, doi: 10.3390/membranes10100254.